

AD-A164 504

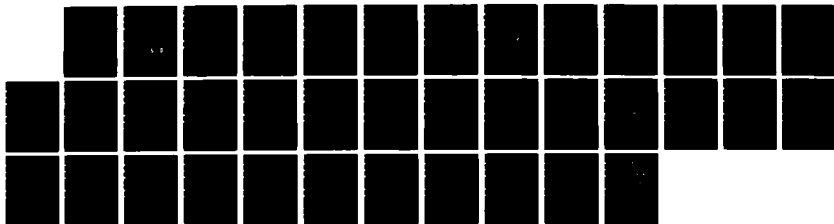
RESEARCH IN SOLAR-TERRESTRIAL PHYSICS(U) CALIFORNIA  
UNIV LOS ANGELES R L MCPHERRON 25 JAN 86  
N00014-84-C-0158

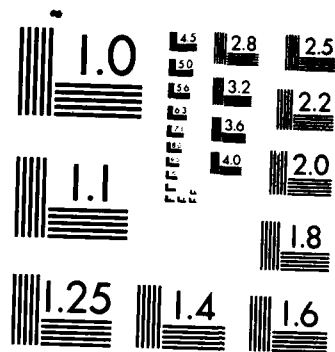
1/1

UNCLASSIFIED

F/G 3/1

NL





MICROCOPY RESOLUTION TEST CHART  
NATIONAL BUREAU OF STANDARDS-1963-A

12

AD-A164 504

Final Technical Report

to

Department of the Navy  
Office of Naval Research

for

"Research in Solar-Terrestrial Physics"

Contract No. N00014-84-C-0158

Project Period: December 1, 1983 - March 31, 1985

Contract Award: \$81,774

Scientific Program Officer: R. G. Joiner, Code N00014

Principal Investigator: R. L. McPherron

by

The Regents of the University of California  
University of California, Los Angeles  
405 Hilgard Avenue  
Los Angeles, California 90024

Date Submitted: January 25, 1986

DTIC  
ELECTE  
S FEB 21 1986 D

DISTRIBUTION STATEMENT A

Approved for public release  
Distribution Unlimited

DTIC FILE COPY

86 0 1 010

## LIST OF FIGURES

<u>Figure</u>		<u>page</u>
1.	Summary of dimensional analysis results for UT parameter. . . . .	4
2.	Comparison of observed and predicted Dst index during first CDAW-6 interval. . . . .	6
3.	Filters which predict polar cap potential. . . . .	8
4.	Comparison of the predicted and observed AL index during the second CDAW-6 interval. . . . .	10
5.	Effects of the IMF on the onset of substorm expansion phase. A possible case of internal triggering. . . . .	13
6.	A comparison of Joule heating rate with solar wind input. . . . .	16
7.	Interpretation of magnetic field observations during 1054 UT March 22, 1979 substorm. . . . .	18
8.	Schematic of currents causing expansion phase magnetic perturbations. . . . .	20
9.	Expected harmonic amplitudes at synchronous orbit. . . . .	23
10.	Observed harmonic amplitudes at synchronous orbit. . . . .	24

Accession For	
NTIS CRA&I	<input checked="" type="checkbox"/>
DTIC TAB	<input type="checkbox"/>
Unannounced	<input type="checkbox"/>
Justification	
By <i>etc. or file</i>	
Distribution /	
Availability Codes	
Dist	Avail and/or Special
A-1	

## CONTENTS

	<u>page</u>
2. . . . .	2
Solar Wind--Magnetosphere Coupling . . . . .	2
Dimensional analysis of energy transfer . . . . .	2
Predicting the storm time ring current . . . . .	5
Predicting the Polar Cap Potential . . . . .	7
Application of Activity Predictors to CDAW-6 Observations . . . . .	9
Roles of driven and loading/unloading processes in substorms . . . . .	11
Substorm Triggering by the Interplanetary Magnetic Field . . . . .	11
Studies of the Near-Earth Plasma Sheet . . . . .	14
Dynamics of an isolated substorm . . . . .	14
Magnetotail energy storage and release during substorms . . . . .	15
Changes in the plasma sheet magnetic field during substorms . . . . .	17
Changes in the Synchronous magnetic field during substorms. . . . .	19
Ultra Low Frequency Waves . . . . .	21
Pc-3 magnetic pulsations . . . . .	21
Software Development . . . . .	25
Flatfile software . . . . .	25
Flat file transfer protocols . . . . .	25
High level software . . . . .	26
 Bibliography of Published Papers	 27

## 1. PROGRAM SUMMARY

The Space Science Group of the Institute of Geophysics and Planetary Physics at the University of California, Los Angeles, is studying the causes of geomagnetic activity as manifested in ULF waves, magnetospheric substorms, and magnetic storms. Our research program utilizes a large body of magnetic data acquired by spacecraft in the solar wind, magnetosphere, and on the earth's surface, as well as correlative information provided by other instruments at the same locations. The primary goal of our research is to understand the physical phenomena which transfer energy from the solar wind to the magnetosphere, which transport this energy within the magnetosphere, and finally which lead to its dissipation in the ionosphere and its return to the solar wind.

Our current research projects include three distinct topics: solar wind-magnetosphere coupling, triggering of substorm expansion onsets, and generation of ultra low frequency waves. Our investigation of solar wind-magnetosphere coupling is concerned with establishing how the rate of energy transfer into the magnetosphere depends on bulk parameters of the solar wind. Also, it involves a study of how this energy is dissipated internally by the auroral electrojets, the ring current, and plasmoids in the magnetotail. Our work utilizes linear prediction filters to characterize the way in which various magnetic indices are controlled by the solar wind.

The second topic, triggering of substorm onsets, is concerned with understanding the mechanism whereby solar wind energy stored in the tail lobes is released into the inner magnetosphere. In the model we favor, this release is caused by reconnection of lobe magnetic field at a near-earth neutral line. Our present research is concerned with demonstrating that this process is highly localized, transient, and at times involves multiple neutral lines. Also, we are trying to determine whether this process is triggered by internal changes or requires an external stimulus.

The third topic is the study of ultra low frequency waves (ULF) (1-1000 mHz). These waves are generated by a variety of mechanisms, some of which depend directly on the solar wind, while others are a consequence of changes associated with substorms and storms. The subject of our current research is a ULF phenomenon occurring on the dayside of the earth and referred to as Pc-3 pulsations (10-45s period). These pulsations are apparently generated by field-line resonances driven by waves produced by the solar wind interaction with the magnetosphere. Our past work shows that these waves may be used to indirectly measure the total mass density of the plasma in the magnetosphere, enabling us to study changes in magnetospheric plasma associated with substorms and storms.

## 2.1 SOLAR WIND--MAGNETOSPHERE COUPLING

A major goal of our current research program is the development of methods of predicting geomagnetic activity from measurements of the solar wind. Practically, such predictions would provide users of geomagnetic indices with sufficient warning that they could modify their equipment or procedures to avoid problems caused by severe substorms or major storms. Scientifically, such predictions would provide insight into the physical processes which generate magnetic activity. Recently, this area of research has come to be known as "solar wind-magnetosphere coupling." Our investigations of this subject are discussed in the following subsections.

### 2.1.1 Dimensional analysis of energy transfer

A major unsolved problem of solar-terrestrial physics is, determining the functional dependence of the rate of solar wind energy transfer into the magnetosphere on interplanetary and magnetospheric parameters. Perreault and Akasofu (1978) suggested this dependence was of the form  $U_T = \epsilon(t)$  where  $U_T$  is the total rate of magnetospheric dissipation and  $\epsilon$  is proportional to  $VB^2 \sin^4 \theta/2$ . Since  $U_T$  depends both on the rate of change of Dst (ring current injection and decay) and on AE (particle precipitation and Joule heating) it would be surprising if the relation were so simple. As discussed in Section 2.1.2 below, our work with Dst demonstrated that the rate of change of Dst is quite predictable from the solar wind electric field (Burton et al., 1975). Also we recently established that the AL index is more closely related to the electric field than it is to  $\epsilon$  (Clauer et al., 1981).

A method for determining which solar wind parameter is the best predictor of a given index of energy dissipation has been suggested by Vasyliunas et al. (1982). This method is based on the principle of dimensional similitude which requires that any magnetospheric dissipation parameter (P) be proportional to the solar wind kinetic energy flux multiplied by some function of the dimensionless parameters involved in the coupling. For an electromagnetic interaction (reconnection) these parameters include the orientation angle of the IMF and the solar wind Mach number. Thus,

$$P = \rho V^3 l_{CF}^2 F(M_A^2, \theta)$$

where  $\rho$  = density,  $V$  = velocity,  $l_{CF}$  = distance to subsolar point. A simple approximation to  $F$  is of the form

$$F = (M_A^2)^{-\alpha} G(\theta)$$

which leads to the relation

$$P = B^{2\alpha} \rho^{2/3-2\alpha} V^{7/3-2\alpha} G(\theta)$$

The preceding relation can be written in the form

$$\log (P/\rho^{2/3} V^{7/3}) = \alpha \log (M_A^{-2}) + \log G(\theta)$$

Providing the solar wind parameters are constant and dissipation has reached equilibrium, observations may be separated into different data sets corresponding to various IMF orientations. Then a plot of the L.H.S. of the preceding relation versus  $M_A^{-2}$  should be a straight line with slope corresponding to the optimum coupling exponent.

We have applied this method to both the total energy parameter  $U_T$  and the electrojet index AE. Figure 1 illustrates the results when the IMF orientation was selected in the range  $-90^\circ \leq \theta \leq -75^\circ$ . A least square, linear fit to the data gives a slope of 0.41 and a correlation coefficient of 0.68. Similar results were obtained for all angles up to  $+30^\circ$ , with a slope 0.5 being most probable. For the AE index, a slope of 0.3 is most probable. These results imply that the optimum coupling parameter for  $U_T$  is

$$U = \rho^{1/6} V^{4/3} B = (\rho V^2)^{1/6} (VB) G(\theta)$$

This parameter is very close to the electric field parameter used by Burton et al. (1975) and quite different from the epsilon parameter advocated by Akasofu (1981b) and Kan and Akasofu (1982). For AE we obtain

$$AE = \rho^{1/3} V^{5/3} B^{2/3}$$

This parameter is closer to electric field than is epsilon but is more like the  $V^2 B$  dependence found empirically by several authors (e.g. Murayama, 1982).

A paper describing these results was presented at an international symposium in Graz, Austria (A-94), and a manuscript has been published in the proceedings (B-69).



# ESTIMATION OF COUPLING EXPONENT

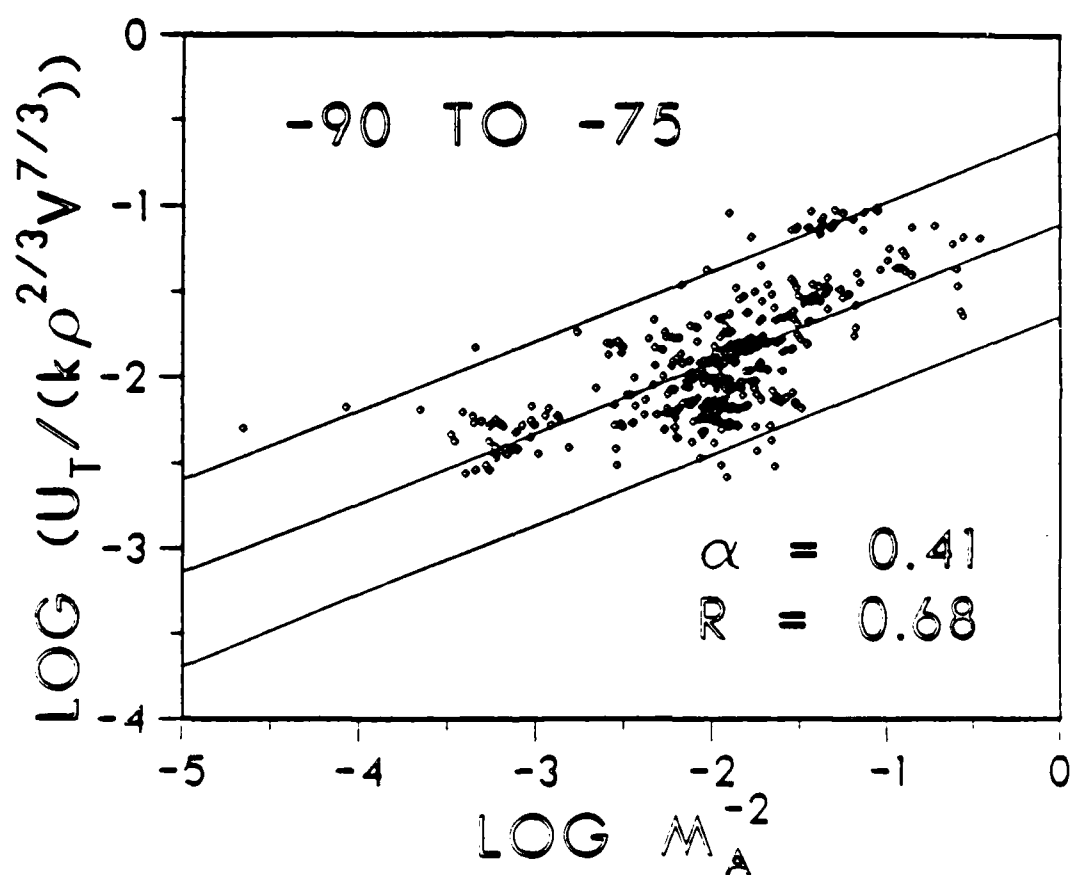


Figure 1: Summary of dimensional analysis results for UT parameter. The ordinate displays the optimum exponent to be used in the solar wind-magnetosphere energy coupling equation

$$P = k B_o^{2\alpha} \rho^{2/3-\alpha} V^{7/3-2\alpha} G(\theta)$$

The abscissa denotes different ranges of the IMF orientation angle.

## 2.1.2 Predicting the storm time ring current

Magnetic storms are disturbances in the earth's magnetic field produced by the drift of particles in a large doughnut-shaped volume circling the earth. These particles are injected into trapped orbits from the tail by time varying magnetospheric electric fields, and from the ionosphere by field aligned potential drops. They are lost from these orbits by precipitation into the atmosphere through charge exchange and wave-particle interaction. Because intense substorms accompany the growth of this "ring current" it has been customary to attribute particle injection to these substorms (Davis and Parthasarathy, 1967). More recent work by Perreault (1974), and by ourselves (Burton et al., 1975), however, shows that the Dst index (a linear measure of the energy in the ring current) is very closely related to the solar wind electric field. As discussed by Harel et al. (1981), this suggests that ring current injection is more properly considered a "convection" phenomenon driven by the solar wind than a "substorm" phenomenon.

We have attempted to determine which of these is more important using the technique of linear prediction filtering. Applying the same procedures as in our AL study (B-44) and our ASYM study (B-48) we have calculated a prediction filter relating the solar wind electric field and the Dst index. Because the filter must represent both rapid injection and slow decay it is necessary to use a very long filter and the highest possible time resolution. In addition, because the Dst index includes effects of magnetopause currents, it is necessary to correct for movement of these currents in response to the solar wind dynamic pressure. This was done by calculating a prediction filter relating Dst and dynamic pressure and subtracting its prediction from the observed index. This residual should contain only the effects of solar wind electric field.

Our results show that the dynamic pressure filter is approximately a delta function, while the electric field filter is a pulse which rises to a peak after only one hour, and which decays slowly to background sometime after 16 hours. Separately, the pressure filter accounts for 12% of the Dst variance, and the electric field filter 45%, while together, they account for 72% of the variance. An example illustrating the quality of the predictions is presented in Figure 2. As apparent from the comparison with observations in the bottom panel, there are significant residuals. These appear to arise from a variety of sources including errors in measurement of the upstream parameters, the definition of the quiet day used in calculating the observed Dst index, and deviations of the decay rate from the average represented by the filter.

Initial results of this work are contained in a paper presented at the COSPAR meeting in Graz (A-97; B-68). A manuscript describing the complete investigation is in preparation.

# COMPARISON OF OBSERVED AND PREDICTED $D_{st}$ INDEX

March 21-23, 1979

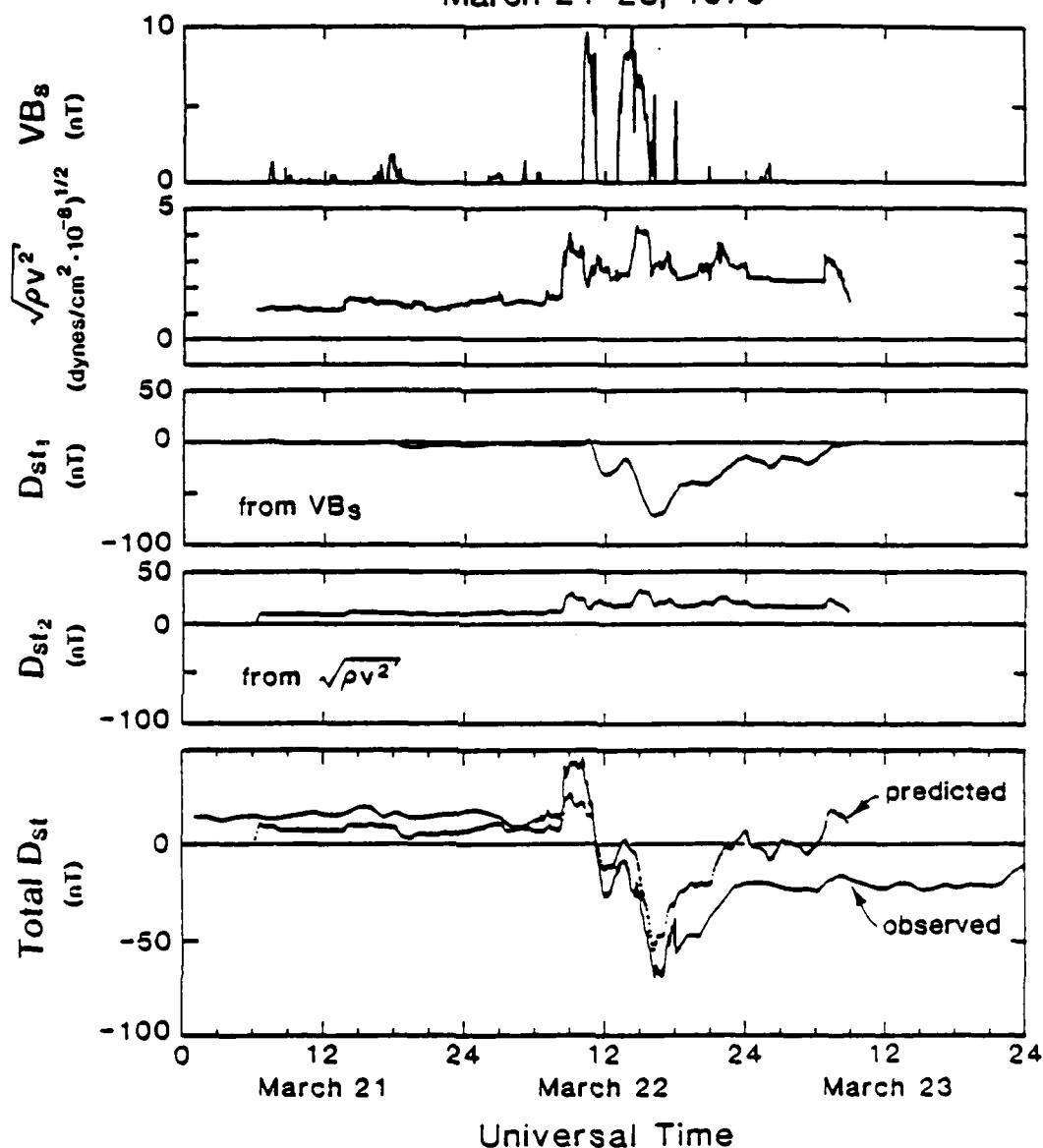


Figure 2: Comparison of observed and predicted  $D_{st}$  index during first CDAW-6 interval. Top two panels show the solar wind electric field and dynamic pressure. Center two panels show the respective contributions of these two sources to  $D_{st}$ . Bottom panel presents observed (solid) and predicted (dotted)  $D_{st}$  index.

### 2.1.3 Predicting the Polar Cap Potential

Our past efforts to predict magnetic activity have made use of magnetic indices because they are so readily available. A potential objection to this use is that the indices are only indirectly related to the underlying physical processes. An opportunity to use more physical parameters has been provided by several recent workshops (Kamide et al., 1982; McPherron and Manka, 1985). In these workshops a large collection of ground magnetic observations have been analyzed to produce a model of "true" ionospheric currents, field aligned currents, ionospheric electric field and Joule heating.

In our study of these data, we began by calculating and comparing prediction filters for AU and AL and their corresponding physical parameters, eastward and westward current strength. Within the constraints of the limited amount of data available for the study, we cannot distinguish between the corresponding pairs of filters. This suggests that our previous work based on the indices alone has not led to inappropriate conclusions as a result of the imperfect way in which the indices monitor the underlying physical quantities.

Our results for the polar cap potential are more interesting, however, because this potential is used extensively by the Rice group as input in a numerical simulation of magnetospheric convection (cf., Harel et al., 1981). In the past, polar cap potential has been calculated from a simple time-independent model of the relation between polar cap potential, and solar wind (Reiff et al., 1981). An empirical model which takes into account the time delays in the magnetospheric response should be helpful in improving these simulations. Also, these delays may provide insight into the physical processes involved in the interaction.

Our results are shown in Figure 3. Two filters are required to predict this potential. The first is for the rectified solar wind electric field, while the second is for the square of the solar wind velocity. The latter, which has the form of a delta function, is required to predict the observed potential drop during times of northward IMF. The form of filter which transforms solar wind electric field to polar cap potential is difficult to perceive because of noise in the filter estimates. It appears to rise to a maximum at 40 minutes and decay to zero after 90 minutes. The steady state response to a 1 mV/m electric field is 20 keV. For comparison, the resting potential for an extremely slow solar wind ( $v = 200$  km/sec) and northward IMF would be 10 keV. For more typical conditions (5 mV/m and 400 km/sec) the values are 100 keV and 40 keV, respectively. While the effect of the electric field is strongest, the effect of the velocity (viscous interaction) is very important.

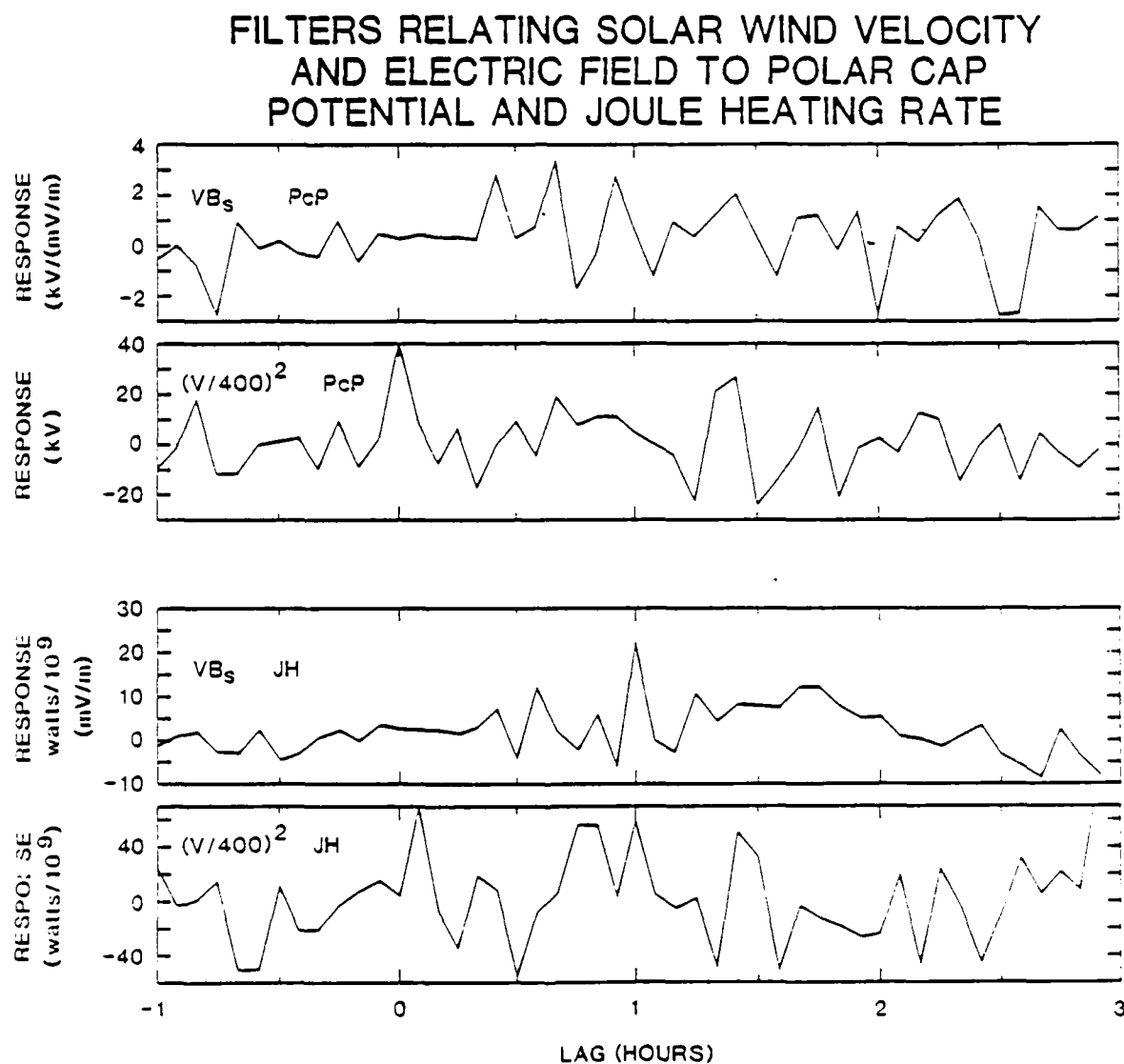


Figure 3: Filters which predict polar cap potential. Top panel shows solar wind electric field filter. Bottom panel shows velocity filter.

#### 2.1.4 Application of Activity Predictors to CDAW-6 Observations

Our empirical technique for predicting geomagnetic activity utilizes past observations to define a system response function which is then convolved with a later input to "predict" the output. If this input is the same as used to define the response function, the output is not truly a prediction. Unless the underlying system is approximately linear and time invariant, this function is only a "representation" of a particular set of data. If, however, the result of convolution with an arbitrary input is reasonably close to the observed output, then the response function may be considered a predictor as well.

In order to test the predictive value of the response functions calculated in our previous studies, we have performed "predictions" for two-three day intervals which encompass the events chosen for study in the Coordinated Data Analysis Workshop, CDAW-6 (see Section 2.2 below). These intervals were chosen because the CDAW-6 workshops have provided a generally accepted morphology with which the residuals in our predictions can be compared. Also, high time resolution magnetic indices based on a large number of stations were available for comparison with the predictions.

The test was carried out in two stages. First, the 52-day data set from 1967-68 was averaged to 5-minute resolution to correspond to the resolution of the CDAW-6 solar wind data. Impulse response functions for all four indices were then calculated at this resolution and plotted. Next, these functions were convolved with the CDAW-6 solar wind input to predict each index. Finally, the observed indices were plotted on top of the predictions for comparison. Figure 4 is an example of such a comparison.

In summary, we find the AU index is least predictable (~20%), AL and ASYM moderately predictable (~40%) and Dst most predictable (~72%). We also find there is virtually no difference between the residuals in the data used to define the response functions and the CDAW-6 residuals suggesting the response functions truly represent physical properties of the system. We attribute the residuals in the Dst index to errors in the input data, to problems defining quiet base lines and finally to an inability to accurately define the decay rate of the ring current. The latter is probably a consequence of ionic composition depending on the level of activity. We attribute the residuals in AL to a lack of a deterministic relation between the solar wind and the exact time and amount of energy released from the tail during a substorm expansion. Our inability to predict the AU index is difficult to understand and suggests the eastward electrojet, which it measures, depends strongly on parameters other than the solar wind electric field.

These results have been presented at a recent meeting in Graz, Austria (A-97) and have been published in the proceedings of that meeting (B-68).

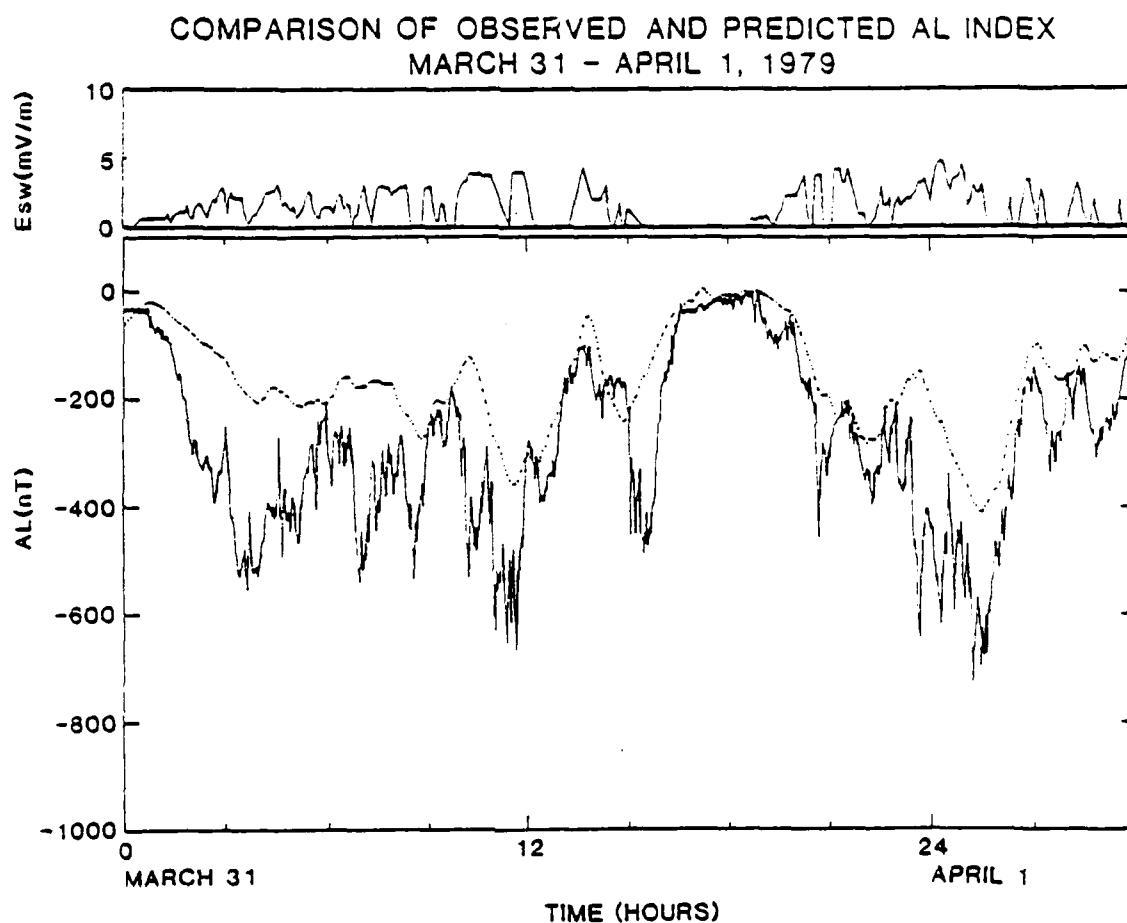


Figure 4: Comparison of the predicted and observed AL index during the second CDAW-6 interval. Top panel shows the solar wind electric field. Bottom panel displays predicted (dotted line) AL index. Note that sudden decreases in AL are not predictable.

### 2.1.5 Roles of driven and loading/unloading processes in substorms

For over a decade it has been known that the magnetotail plays a major role in magnetospheric substorms. As outlined by McPherron et al. (1973) and Russell and McPherron (1973), this role is to accumulate energy from the solar wind-magnetosphere interaction and to later release this energy in bursts called substorms. Recently, an alternative model has been suggested by Akasofu (1981a) in which substorm phenomena are explained as manifestations of field aligned and ionospheric currents directly driven by the solar wind-magnetosphere interaction. In this model the only role of the magnetotail is to determine the size of the polar cap, and hence, the location of disturbances in the ionosphere. Akasofu (1979) characterizes these alternate models as "loading/unloading" systems and "driven" systems respectively. In numerous publications (e.g. Akasofu, 1981b) he has argued that the magnetosphere is primarily a driven system and that the magnetotail plays a passive role.

The importance of driven processes in magnetospheric dynamics is implicit in the loading/unloading model of substorms. The process of energy storage involves merging of interplanetary magnetic field with the earth's field and transport of dayside magnetic flux to the tail lobes. Subsequently, the field lines are reconnected and returned to the dayside completing a closed circuit of magnetospheric convection. Field aligned currents generated by this convection close through the ionosphere and produce significant and observable effects. In quasi-steady state there processes are, in fact, the driven system. In the loading/unloading model, however, it is argued that these processes bring about changes in the magnetospheric configuration which ultimately lead to the rapid release of energy accumulated in the tail lobes. Much of this energy is dissipated in the atmosphere as is the case for the driven processes. The question of whether the magnetosphere is primarily a driven or an unloading system is a question of the relative magnitude of the energy dissipation associated with the two types of processes. An attempt to pose this question, and to define driven and unloading processes was made in a manuscript submitted for publication last November (B-50). Also, we have attempted to answer the question by a careful study of several substorms occurring during the CDAW-6 intervals (see subsection 2.2.2 below). A manuscript (B-71) describing this CDAW-6 study has been accepted for publication.

### 2.1.6 Substorm Triggering by the Interplanetary Magnetic Field

In the loading/unloading model of substorms energy extracted from the solar wind is stored in the tail lobes and later released. A variety of mechanisms for initiating this release have been suggested. Among these are solar wind pressure discontinuities (Kokobun et al., 1977) plasma sheet thinning (McPherron et al., 1973), field aligned current instability (Akasofu, 1981a), and northward turnings of the IMF (Caan et al., 1977). The last of these possibilities has attracted recent attention and Rostoker



(1983) and Rostoker et al. (1983) have published several examples of substorms which appear to have been unambiguously triggered by northward turnings of the IMF. These results have led Rostoker to conclude that all major substorm expansions are so triggered (Rostoker et al., 1983).

While it is our own work which led to the identification of IMF triggering, (e.g., Caan et al., 1977, 1978) we do not believe this is the only cause of onset, as it does not explain why the typical delay time between a southward turning and expansion onset is about 60 minutes. This could happen if 60 minutes were the typical duration of southward IMF, but this is not observed. We feel it is far more likely that this delay represents a time scale inherent to the magnetosphere, that is, the time for the tail current to reach an instability threshold.

We have studied the question of IMF triggering by attempting to find unambiguous examples of both IMF and internally triggered onsets. In this investigation we find that there are few such examples. There are several reasons for this. First, the IMF is seldom steady in direction and often fluctuates widely. At such times an apparent correlation can always be made. This is particularly true because it is not obvious when an observed discontinuity should arrive at the earth. Our work shows that several published correlations are probably fortuitous since careful analysis of the propagation of the IMF discontinuity to the earth gives an arrival time different from the expansion onset. Also, we find the concept of "discontinuity" ambiguous as well. In several examples of expansion onset during what we consider "steady" IMF, Rostoker (personal communication) has pointed out exceedingly small changes in slope (i.e. constant, to 1 nT/hour northward turning as the probable trigger. Figure 5 depicts such a situation.

In view of the foregoing we conclude that it is not possible to decide whether or not triggering by the IMF occurs with the data available to us for this study. Our preliminary results were presented at the December 1983 AGU meeting (A-95) and a draft manuscript has been completed.

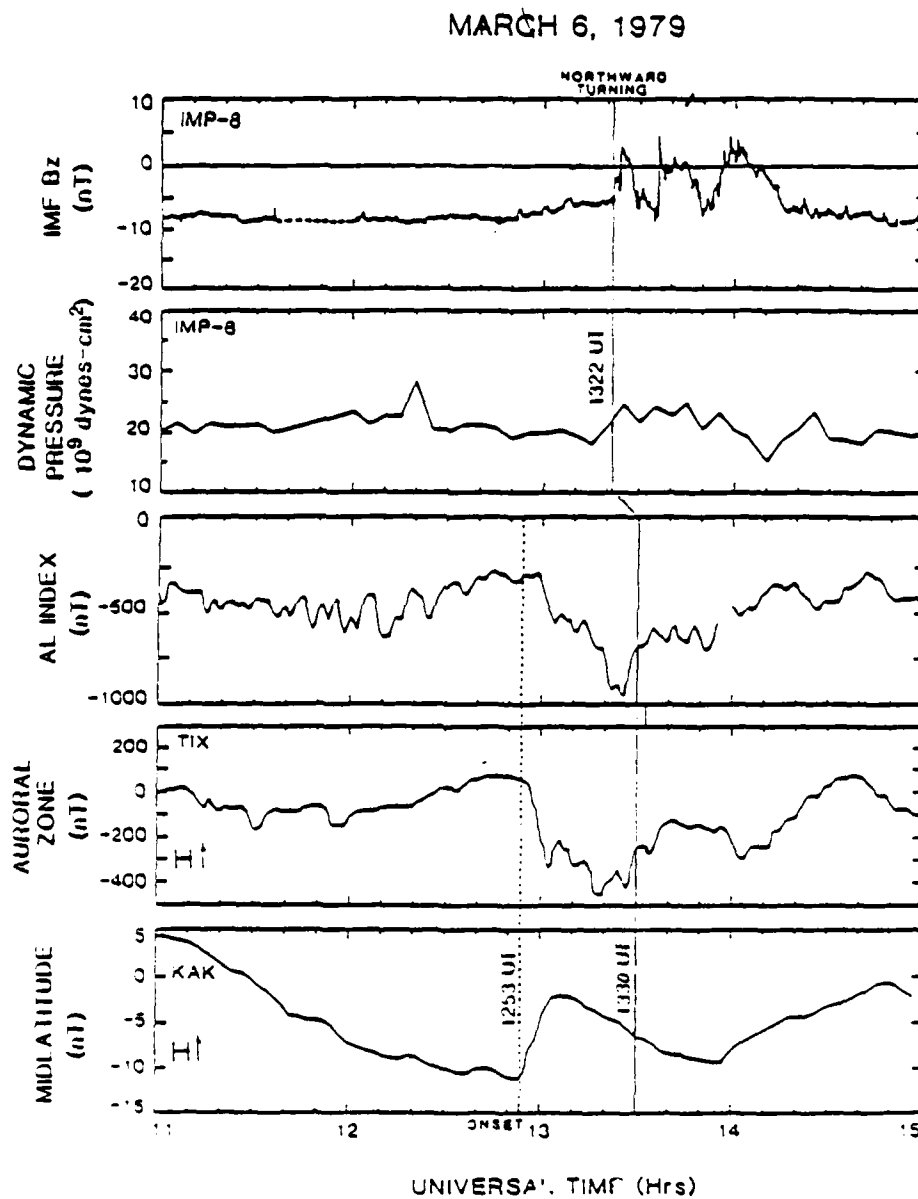


Figure 5: Effects of the IMF on the onset of substorm expansion phase. A possible case of internal triggering.

## 2.2 STUDIES OF THE NEAR-EARTH PLASMA SHEET

### 2.2.1 Dynamics of an isolated substorm

In the past decade there have been a number of papers describing detailed time histories of magnetospheric substorms (e.g. McPherron et al., 1973; Nishida and Kamide, 1983). The primary goal of these studies has been to determine the physical processes by which energy and particles are transferred from the solar wind to the magnetosphere and transported within to final deposition in the ionosphere. With the introduction of the Coordinated Data Analysis Workshops (CDAW) (Vette et al., 1982), such studies have become increasingly detailed. In CDAW workshops data from many spacecraft and ground observatories are combined in a digital data base and jointly studied by a number of investigators from many countries.

Several years ago we initiated the investigation of two intervals of substorm activity in a sequence of workshops which have been named CDAW-6. In this investigation the primary emphasis has been an isolated substorm which followed an interval of magnetic quiet, and during which the ISEE 1/2 spacecraft were inbound in the near-earth plasma sheet. Fortunate circumstances placed the spacecraft on the central meridian of the disturbance, and also in the plasma near the center of the neutral sheet at the time of expansion onset.

Our major contribution to this study has been an overview of the event establishing the time history of the substorm, and the general correspondence of the observations to the "neutral-line" model of substorms. In our opinion, the gross behavior of the magnetic field and plasma supports the idea that magnetic merging on the dayside enables the solar wind to transport dayside magnetic flux to the lobes of the tail. A concurrent return of flux exhausts the plasma sheet as simultaneously the lobe flux increases. Eventually, the near-earth plasma sheet thins to the point that reconnection begins, diverting a portion of the enhanced tail current to the ionosphere. When the merging process encounters open field lines of the lobe, a plasmoid is formed and pulled from the tail by reconnected field lines of the solar wind. Merging continues until quenched by exhaustion of available energy, or by a relaxation of solar wind stress (northward turning of IMF). At this point the neutral line moves rapidly tailward expanding the plasma sheet.

Although the gross behavior of plasma and field seems consistent with this model, opponents of this view have raised a number of questions, particularly with behavior of more energetic particles in the plasma sheet boundary layers. In our opinion, these can be explained by the formation of multiple neutral lines in different azimuthal and radial sectors at different times in the substorm. Unfortunately, these assumptions cannot be verified with the available data, and opponents of the neutral line model remain unconvinced.

Our description of the dynamics of this substorm has been presented in papers at several meetings (A-79, A-85). A manuscript describing the results has been accepted for publication (B-64). Our paper will appear as the lead paper in a set of approximately 20 papers in the Journal of Geophysical Research, February 1985.

## 2.2.2 Magnetotail energy storage and release during substorms

One of the outstanding questions concerning substorms is the relative importance of driven and loading/unloading processes. As discussed above in Section 2.1.5, it is now evident that both processes contribute to substorms, however, which process produces the most energy dissipation cannot be determined from studies of magnetic indices. According to Akasofu (1981b) the similarity between the solar wind energy parameter  $\epsilon$  and the AE and  $U_T$  indices implies that the magnetospheric system is predominantly driven. However, as we have pointed out, if the release of energy from the magnetotail is a consequence of solar wind induced changes in the tail, the effects of the release will also be correlated with the solar wind.

One way of addressing the question of relative importance is to compare physical measures of energy dissipation at times when only one or the other of the two processes is operative. An opportunity to make this comparison was provided by the CDAW-6 data base described in section 2.2.1. The large collection of ground magnetic data (Kamide et al., 1983) made it possible to model ionospheric currents and the Joule heating they caused. Also, an accurate Dst provided a measure of dissipation due to ring current injection. The same data also provided the information needed to define substorm phases, in particular expansion onsets which are generally thought to be caused by release of energy from the tail. Finally, the availability of satellite data made it possible to determine the state of the magnetotail.

Our study shows that the time history of Joule heating during a substorm has two components. The first begins soon after a southward turning of the IMF, the second shortly after the onset of an expansion phase. In cases where the IMF remains rather steadily southward, the Joule heating curve returns to the pre-expansion level after about one hour. This behavior suggests the first component is the driven component while the latter is the unloading component. Figure 6 illustrates this behavior for a short- and a long-duration event.

A comparison with other data indicates that the second component occurs after expansion phase onset, and in coincidence with dipolarization of the field at synchronous orbit and a decrease in tail lobe field intensity.

From the figure, it is evident that the magnitude of the Joule heating rate after expansion onset is 4-5 times as large as that before or after. Extrapolating the pre-onset values to later times and integrating the area under this curve gives a total heating due to the "driven" component.

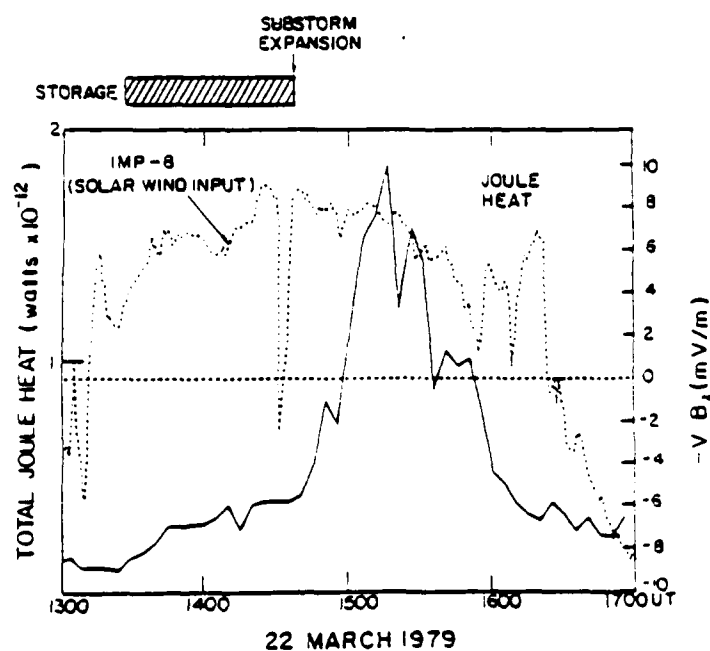
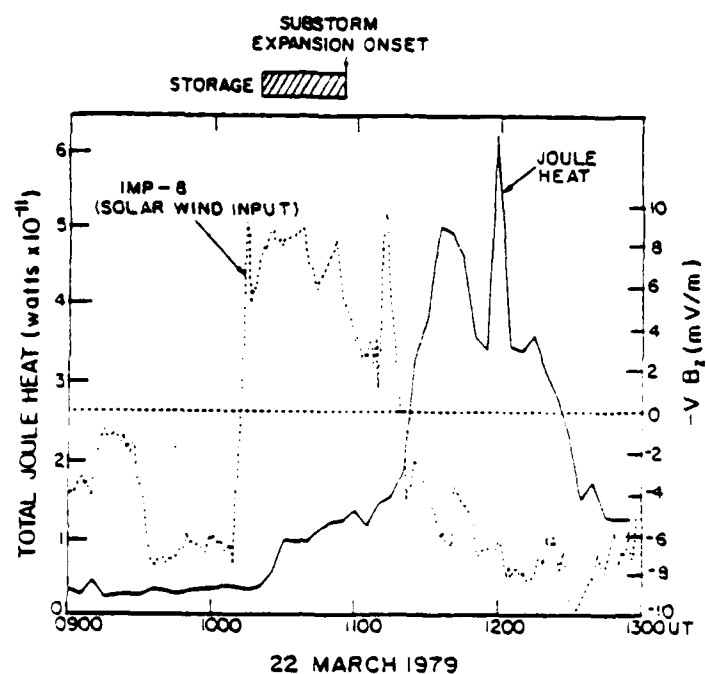


Figure 6: A comparison of Joule heating rate with solar wind input. Heating rate is much less than during expansion phase.  
 (a) Short duration event with expansion onset at 1055 UT.  
 (b) Long duration event with onset at 1436 UT.

Subtracting this from the total integral gives the component due to unloading. We find that the unloading component dissipates 2-5 times as much energy as the driven component.

### 2.2.3 Changes in the plasma sheet magnetic field during substorms

As part of the CDAW-6 investigation described in Section 2.2.1, we have carried out a detailed study of the plasma sheet magnetic field. The motivation for this study was the observation that shortly after onset the field at the neutral sheet was directed southward with magnitude  $\sim 60$  nT and that it was accompanied by a rapid tailward flow of plasma. Such behavior is expected tailward of a neutral line which in this case must have formed earthward of  $-14$  Re.

Our ability to observe this event is a consequence of special circumstances of dipole, spacecraft and solar wind geometry. At the time of the event, 1055 UT March 22, 1979, the dipole axis was almost exactly perpendicular to the earth-sun line so that the neutral sheet should be located in the GSM equatorial plane, with the spacecraft  $\sim 1$  Re south of it. Fortunately, however, the southward turning of the IMF which generated the substorm was accompanied by a southward turning of the solar wind velocity vector. Later, the northward turning of the IMF was accompanied by a corresponding northward change in velocity. These changes, combined with waves on the neutral sheet, caused multiple crossings of the neutral sheet which were observed by both ISEE spacecraft. Using time delays between the two spacecraft we have been able to estimate the velocity and thickness of the plasma sheet, as well as transform the magnetic data to an appropriate "tilted" neutral sheet coordinate system.

Our results show that at the beginning of the substorm the current sheet was quite thick. However, as the growth phase progressed it rapidly thinned. Immediately after expansion onset it became so thin ( $\leq 1000$  km) that the two spacecraft were on opposite sides of the sheet for almost 15 minutes. Furthermore, the weakly southward IMF seen throughout this interval by both spacecraft was truly a southward field and not an effect of tilting of the neutral sheet. Finally, timing of the intense southward field at the two spacecraft suggests that a plasmoid was ejected from the near-earth region with a velocity comparable to the plasma streaming velocity (500 km/sec).

A paper describing these observations has been presented at two meetings (A-80, A-86) and a manuscript is under preparation. Figure 7 summarizes our interpretation of changes in field configuration at various times.

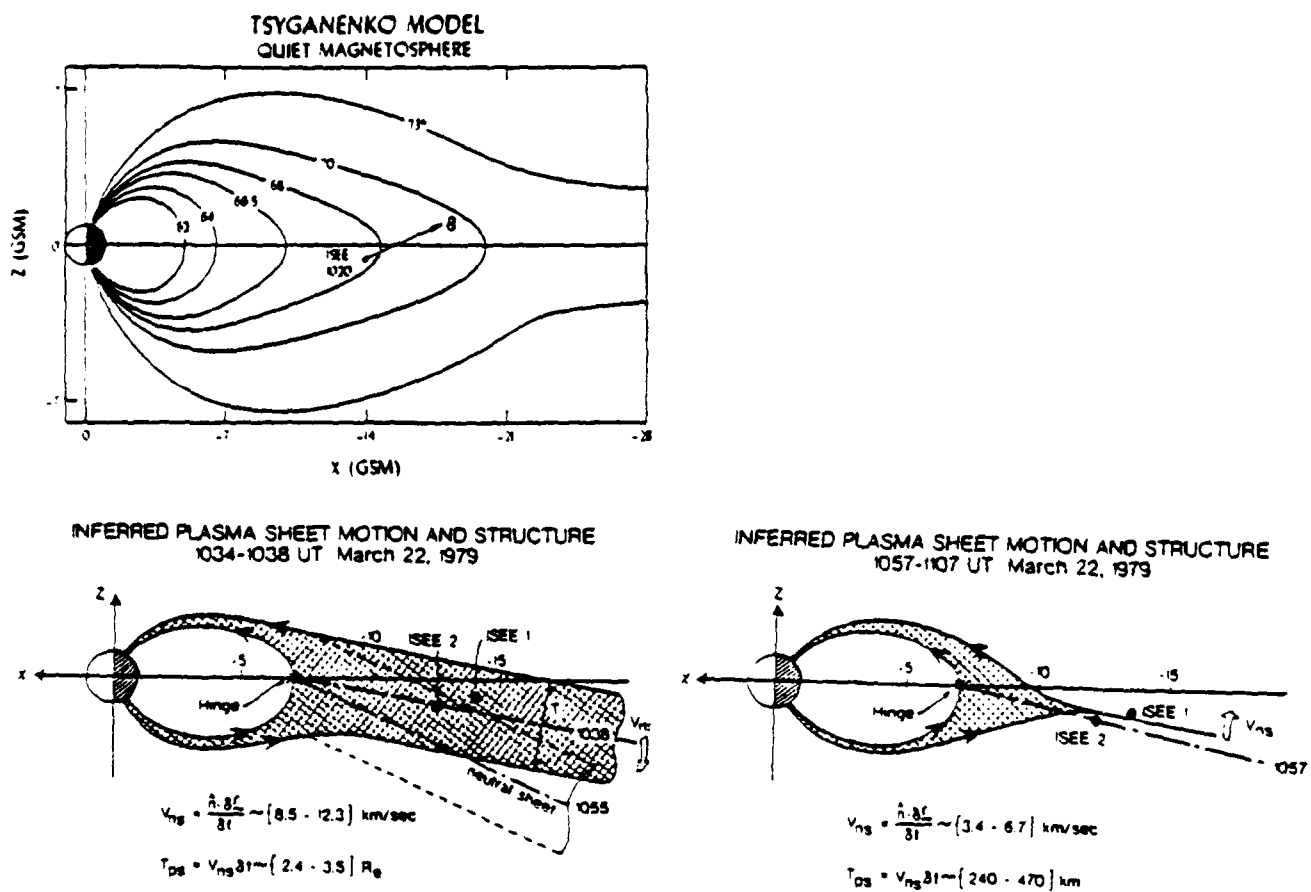


Figure 7: Interpretation of magnetic field observations during 1054 UT March 22, 1979 substorm. Top left panel shows possible quiet time plasma sheet configuration. Bottom left panel shows configuration immediately before onset. Upper right panel shows configuration shortly after onset.

## 2.2.4 Changes in the Synchronous magnetic field during substorms.

During the CDAW-6 substorms of March 22, 1979, two synchronous spacecraft carrying magnetometers passed through the midnight sector. As we have shown previously (Kokobun and McPherron, 1981) the synchronous magnetic field exhibits a "two phase" behavior during substorms. During the growth phase, the field orientation becomes increasingly tail-like, while during the expansion phase it becomes more dipolar.. Baker et al. (1978) have reported similar behavior from energetic particle anisotropies at synchronous orbit and suggest that such measurements can be used to predict the occurrence of substorm expansions. Nagai (1982) has extended these observations using multiple synchronous spacecraft magnetometers to determine the spatial extent of the "tail-like" and "dipole-like" field changes. He concludes that the former is a result of inward movement and growth of the tail current, while the latter is caused by the rapid eastward and westward expansion of a field aligned current wedge formed at expansion onset.

Using data from the CDAW-6 data base, we have examined the behavior of the synchronous magnetic field during the March 22, 1979 substorms. We find that the earliest indication of expansion onset observed anywhere in the magnetosphere was at a synchronous spacecraft located on a field line very close to the meridian and latitude at which the westward traveling surge formed. Seventeen minutes later, the region of disturbance expanded and a synchronous magnetometer  $30^\circ$  east of the first recorded a dipolarization of the field.

These results support the idea that the region in which the substorm expansion begins is close to the earth and involves a diversion of tail current into the ionosphere. Such a diversion is required for the formation of a neutral line, which is the interpretation we made of the near-earth plasma sheet measurements (c.f. Section 2.2.3). The results also support the suggestion of Nagai that the region of diversion, i.e. the neutral line, expands azimuthally during the substorm expansion phase. A schematic illustration of this current system is presented in Figure 8.

A manuscript describing these results has been submitted for publication as part of the CDAW-6 collection (B-70).



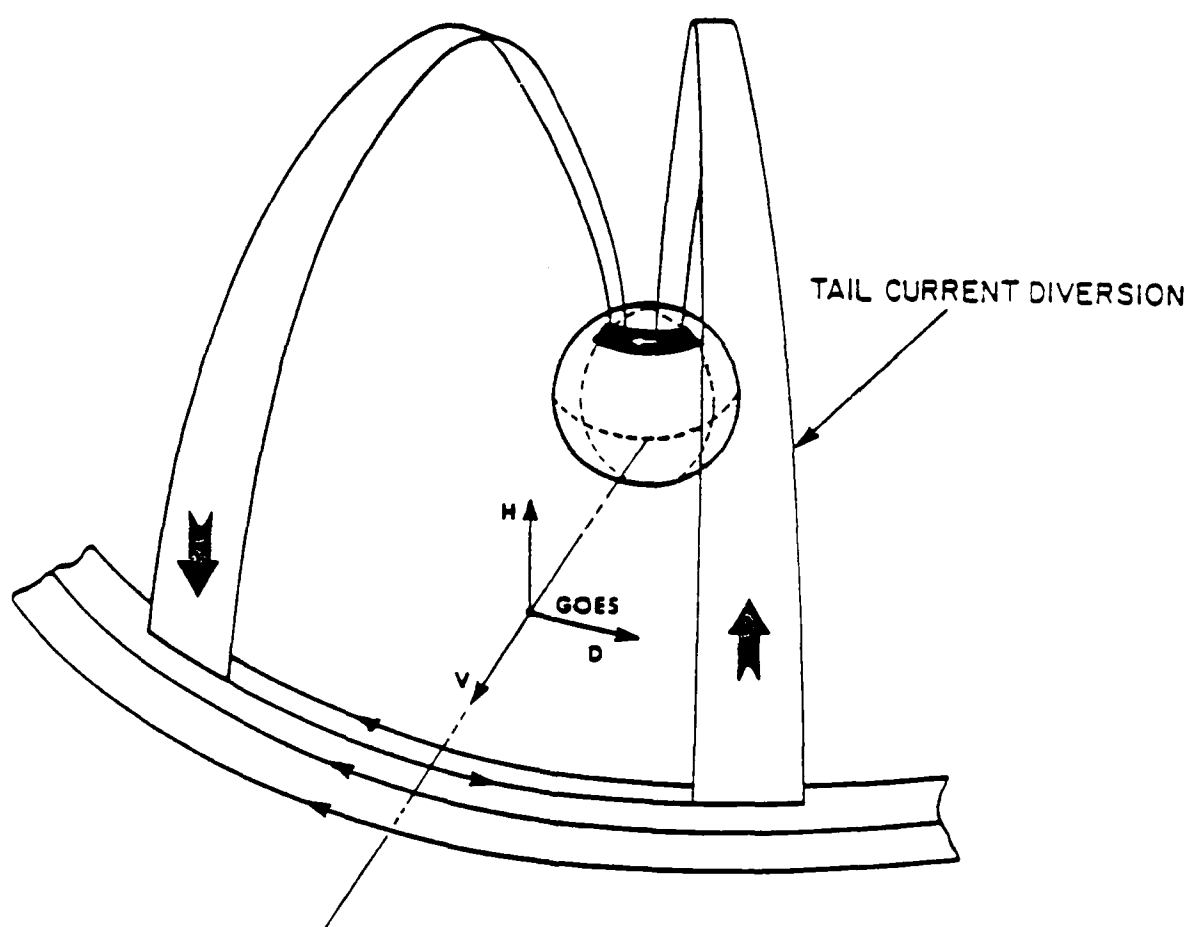


Figure 8: Schematic of currents causing expansion phase magnetic perturbations. The east and west edges expand away from the center as time progresses.

## 2.3 ULTRA LOW FREQUENCY WAVES

Ultra low frequency (ULF) waves are observed throughout the magnetosphere virtually all the time. They are generated by a variety of mechanisms such as field line resonance and plasma instabilities. Because the wave velocities, frequencies, and polarization depend on the magnetic field and plasma conditions in the region of generation, they provide a means of indirect measurement of such quantities. During the past year we have continued our study of these waves, emphasizing Pc-3 pulsations which appear to be generated in the solar wind.

### 2.3.1 Pc-3 magnetic pulsations

Pc-3 (pulsations continuous  $15 < T < 45$  s) are a daytime phenomenon observed both at the earth's surface and in space. Their occurrence is closely controlled by the solar wind velocity and magnetic field orientation (B-39). At synchronous orbit their complex waveform can be resolved into a sequence of harmonic frequency bands, the separation of which gives the total mass density distributed along a field line passing through the spacecraft (B-47). Observations with multiple spacecraft demonstrate that every point in space is oscillating with a different frequency spectrum dependent on local conditions (B-53). The magnetic polarization of these oscillations is always azimuthal, never radial as previously reported (B-55), and corresponds to predictions made by theories of driven field line resonances (Southwood, 1974). Their relation to the solar wind suggests they are generated outside the magnetopause and penetrate through the boundary to drive resonant field line oscillations. To stimulate the broad range of harmonics observed, the input spectrum must be very broad. A suggestion that the period of Pc-3 pulsations is controlled by the magnitude of the upstream solar wind magnetic field (Gul'yel'mi, 1973) does not seem to be true at synchronous orbit. The only observable IMF effects is a slight increase of the amplitude of the highest harmonics with increasing field magnitude (B-54).

During the last year our main activity in the study of Pc-3 pulsations has been to complete a PhD dissertation on this topic (Takahashi, 1983), and to publish the papers summarized in the preceding paragraph. New results contained in the dissertation and not yet published are concerned with the relative amplitude and frequency of harmonics, and the sensitivity of field line eigenfrequencies to boundary conditions field models and plasma models. The observed distribution of the ratio of third to second harmonic frequency is shown in panel a of Figure 9. The peak of the histogram at 1.56 implies that the most probable distribution of plasma mass along a field line is proportional to the fourth power of radial distance. Using this model we have calculated numerically the expected ratio of harmonic amplitudes as a function of latitude, (panel b). For equal excitation, the expected inequality at  $10^\circ$  magnetic latitude is

$$A_5 > A_3 > A_6 > A_2 \gg A_4.$$

Panel a of Figure 10 contains the experimental results where it is apparent that the inequality for median amplitudes is more like  $A_3 > A_2 \gg A_5 \sim A_4$ .

The major discrepancy is that  $A_5$  and  $A_6$  are very much smaller than predicted. A likely explanation for this is that the input spectrum decreases at frequencies above the third harmonic. In fact, as noted above, there is a weak dependence of these harmonic amplitudes on the strength of the IMF.

Another factor which may contribute to this discrepancy is the sensitivity of the location of nodes of the higher harmonics to the distribution of plasma along field lines. For example, as demonstrated in panel b of Figure 10, the location of the fourth harmonic node changes by over  $10^\circ$  depending on the exponent used to characterize the plasma distribution. Also, as shown by the dashed line, the actual latitude of the spacecraft is a function of time, and hence it must move through nodes of higher harmonics throughout the day.

The frequency analysis leads us to the conclusion that our current knowledge of the spacecraft position in the actual magnetic field, and the mass distribution along field lines, are not well enough known to predict relative harmonic amplitudes.

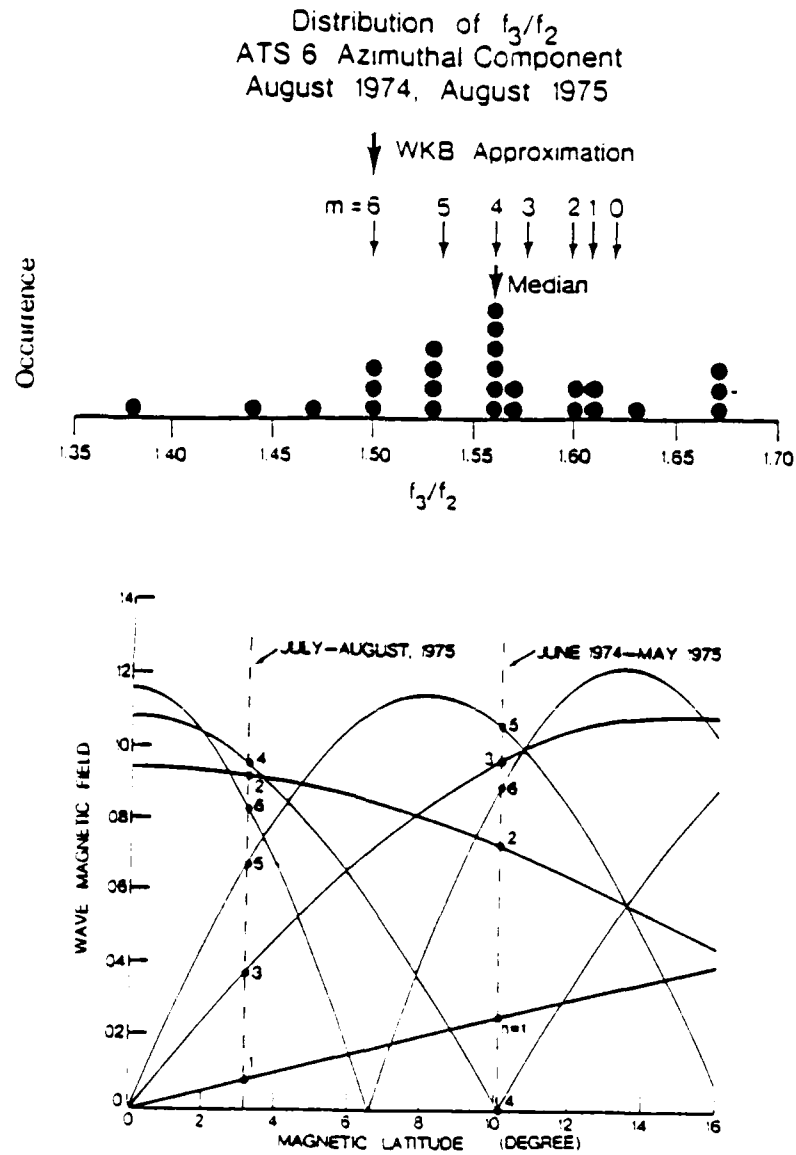


Figure 9: Expected harmonic amplitudes at synchronous orbit. (a) Observed ratio of third to second harmonic frequencies are compared to expectations for different power law distributions of plasma mass density. (b) Calculated wave amplitude as a function of latitude for different harmonics using most probable mass distribution ( $m = 4$ ).

Latitude Dependence of Spectral Density  
in Harmonic Bands  
ATS 6, Azimuthal Component 97

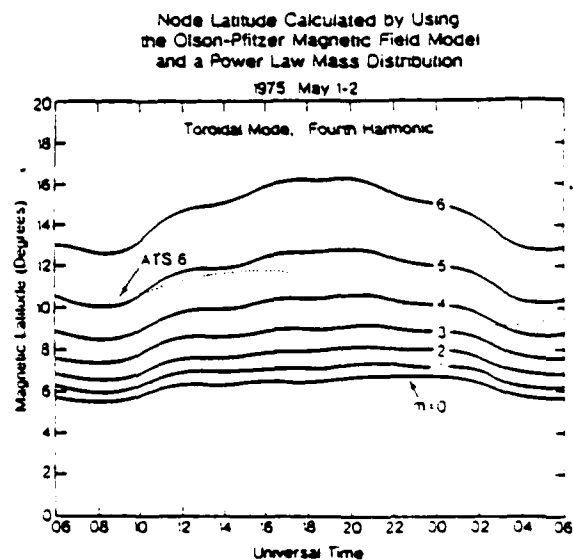
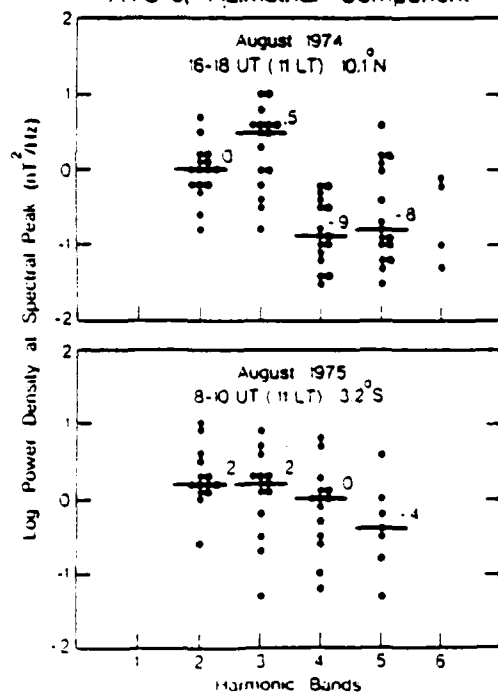


Figure 10: Observed harmonic amplitudes at synchronous orbit.  
(a) Distribution of observed harmonic amplitudes at two different mean spacecraft latitudes. (b) Latitude of fourth harmonic node using model field and plasma compared with trajectory of ATS-6.

## 2.4 SOFTWARE DEVELOPMENT

### 2.4.1 Flatfile software

For several years, the Space Science Group of the Institute of Geophysics and Planetary Physics at UCLA has been developing software to support its activities in management and analysis of time series data. During the past year, we have concentrated on extending this system from the HP minicomputer to an APPLE and an IBM personal computer. The primary objective of this extension is to allow us to acquire and process data at remote locations using interactive software similar to that available in our laboratory.

We have made considerable progress during the reporting interval. We have defined a format--the microcomputer flat file--and developed a number of supporting programs. These include:

1. Flat file keyboard entry
2. Flat file digitizer entry
3. Flat file editing
4. Flat file screen plot
5. Flat file pen plot
6. Flat file printer tabulate
7. Flat file select and merge
8. Flat file statistics

### 2.4.2 Flat file transfer protocols

In order to analyze data acquired at a remote location using a microcomputer such as the APPLE or IBM-PC, it is necessary to transfer floppy disk files to larger computers. During the last year we have acquired and tested protocols from APPLE IIe to IBM-PC, APPLE IIe to IBM 3033, and IBM-PC to IBM 3033. In addition, we have made some progress in developing an APPLE-IIe to HP-1000 protocol. Work is also in progress to allow transfer from the IBM-PC to VAX-780.

### 2.4.3 High level software

Since our last report, we have made progress in transferring some of our analysis programs from the IBM 3033 to a VAX 780. An important element in the transfer has been the acquisition for the VAX of the SPEAKEZ language, a very high-level interpretative language for management and analysis of structured data. We are currently working on the creation of additional modules to tailor the language to our own needs. For example, a Fast Fourier Transform function has been added. As another example, we have also acquired the data management system INGRES and will attempt to interface this file manager to the SPEAKEZ language in a user-transparent fashion.

# ONR BIBLIOGRAPHY OF PUBLISHED PAPERS

1973 to January 1985

1. Snare, R.C., D.J. Peters, P.J. Coleman, Jr., and R.L. McPherron, Digital data acquisition and processing from a remote magnetic observatory, IEEE Trans. Geosci. Elec., GE-11(3), 127-134, 1973.
2. Caan, M.N., R.L. McPherron, and C.T. Russell, Solar wind and substorm related changes in the lobes of the geomagnetic tail, J. Geophys. Res., 78(34), 8087-8096, 1973.
3. McPherron, R.L., C.T. Russell, M.G. Kivelson, and P.J. Coleman, Jr., Substorms in space: The correlation between ground and satellite observations of the magnetic field, Radio Sci., 8(11), 1059-1076, 1973.
4. Russell, C.T., R.L. McPherron, and R.E. Burton, On the cause of geomagnetic storms, J. Geophys. Res., 79(7), 1105-1109, 1974.
5. McPherron, R.L., Critical problems in establishing the morphology of substorms in space, p. 335-347 in Magnetospheric Physics, edited by B.M. McCormac, D. Reidel, Dordrecht, Holland, 1974.
6. Caan, M.N., R.L. McPherron, and C.T. Russell, Substorm and interplanetary magnetic field effects on the geomagnetic tail lobes, J. Geophys. Res., 80(1), 191-194, 1975.
7. Clauer, C.T. and R.L. McPherron, Mapping the local time-universal time development of magnetospheric substorms at midlatitudes, J. Geophys. Res., 79(19), 2811-2820, 1974.
8. Clauer, C.R. and R.L. McPherron, Variability of midlatitude magnetic parameters used to characterize magnetospheric substorms, J. Geophys. Res., 79(19), 2898-2900, 1974.
9. Horning, B.L., R.L. McPherron, and D.D. Jackson, Application of linear inverse theory to a simple current model of the magnetospheric substorm expansion, J. Geophys. Res., 79(34), 5202-5210, 1974.
10. Arthur, C.W. and R.L. McPherron, A preliminary study of simultaneous observations of substorm-associated Pi 2 micropulsations and their high-frequency enhancement, unpublished report, 1974.



11. Caan, M.N., R.L. McPherron, and C.T. Russell, Magnetospheric substorms: A computerized determination and analysis, unpublished report, 1974.
12. Pytte, T., R.L. McPherron, and S. Kokubun, The ground signature of the expansion phase during multiple onset substorms, Planet. Space Sci., 24, 1115-1134, 1976.
13. Pytte, T., R.L. McPherron, M.G. Kivelson, H.I. West, Jr., E.W. Hones, Jr., Multiple satellite studies of magnetospheric substorms: I. Radial dynamics of the plasma sheet, J. Geophys. Res., 81(34), 5921, 1976.
14. Pytte, T., R.L. McPherron, M.G. Kivelson, E.W. Hones, Jr., and H.I. West, Jr., Multiple satellite studies of magnetospheric substorms: Plasma sheet recovery and the poleward leap of auroral zone activity, J. Geophys. Res., 83(A11), 5256-5268, 1978.
15. Kokubun, S., R.L. McPherron, and C.T. Russell, Triggering of substorms by interplanetary discontinuities and the solar wind magnetic field, J. Geophys. Res., 82(1), 74-85, 1977.
16. Burton, R.K., R.L. McPherron, and C.T. Russell, The terrestrial magnetosphere: A half-wave rectifier of the interplanetary electric field, Science, 189, 717-718, 1975.
17. Burton, R.K., R.L. McPherron, and C.T. Russell, An empirical relationship between interplanetary conditions and Dst, J. Geophys. Res., 80(31), 4204-4214, 1975.
18. Pytte, T., R.L. McPherron, E.W. Hones, Jr., and H.I. West, Jr., Multiple-satellite studies of magnetospheric substorms: Distinction between polar magnetic substorms and convection-driven negative bays, J. Geophys. Res., 83(2), 663-679, 1978.
19. Coleman, P.J., Jr. and R.L. McPherron, Substorm observations of magnetic perturbations and ULF waves at synchronous orbit by ATS-1 and ATS-6, p. 345-364 in The Scientific Satellite Program During the International Magnetospheric Study, edited by Knott and Battrick, D. Reidel, Dordrecht, Holland, 1976..
20. Caan, M.N., R.L. McPherron, and C.T. Russell, The statistical magnetic signature of magnetospheric substorms. Planet. Space Sci., 26, 269-279, 1978.
21. Caan, M.N., R.L. McPherron, and C.T. Russell, Characteristics of the association between the interplanetary magnetic field and substorms, J. Geophys. Res., 82(29), 4837-4842, 1977.
22. McPherron, R.L., A self-documenting source-independent data format for computer processing of tensor time series, in Phys. Earth Planet. Int., 12, 103-111, 1976.

23. McPherron, R.L., The analysis and processing of large amounts of geophysical data: Time series data base management, unpublished report, 1976.
24. McPherron, R.L., The use of ground magnetograms to time the onset of magnetospheric substorms, J. Geomagn. Geoelectr., 30, 149-163, 1978.
25. McPherron, R.L., and J.N. Barfield, The disappearance of the effect of substorm field-aligned currents at synchronous orbit near winter solstice, J. Geophys. Res., 85(A12), 6743-6746, 1980.
26. Bossen, M., R.L. McPherron, and C.T. Russell, A statistical study of Pc 1 magnetic pulsations at synchronous orbit, J. Geophys. Res., 81(34), 6083, December 1976.
27. Bossen, M., R.L. McPherron, and C.T. Russell, Simultaneous Pc 1 observations by the synchronous satellite ATS-1 and ground stations: implications concerning IPDP generation mechanisms, J. Atmos. Terrest. Phys., 38, 1157-1167, 1976.
28. Kokubun, S., R.L. McPherron, and C.T. Russell, OGO-5 observations of Pc 5 waves: Ground-magnetospheric correlations, J. Geophys. Res., 81(28), 5141, 1976.
29. Kokubun, S., M.G. Kivelson, R.L. McPherron, C.T. Russell, and H.I. West, Jr., OGO-5 observations of Pc 5 waves: particle flux modulations, J. Geophys. Res., 82(19), 2774, 1977.
30. Clauer, C.R. and R.L. McPherron, On the relationship of the partial ring current to substorms and the interplanetary magnetic field, J. Geomagn. Geoelectr., 30, 195-196, 1978.
31. McPherron, R.L., Magnetospheric substorms, Rev. Geophys. Space Phys., 17(4), 657-681, 1979.
32. McPherron, R.L., Magnetic variations during substorms, p. 631-647 in Dynamics of the Magnetosphere, edited by S.-I. Akasofu, D. Reidel, Hingham, MA 1979.
33. Southwood, D.J. and W.F. Stuart, Pulsations at the substorm onset, p. 341-356 in Dynamics of the Magnetosphere, edited by S.-I. Akasofu, D. Reidel, Hingham, MA 1979.
34. Clauer, C.R. and R.L. McPherron, Predicting partial ring current development, Proceedings of the International Solar-Terrestrial Prediction Workshop, Boulder, Colorado, Vol. 4, B44-B58, March 1980.
35. Arthur, C.W. and R.L. McPherron, Simultaneous ground-satellite observations of Pi 2 magnetic pulsations and their high-frequency enhancement, Planet. Space Sci., 28, 875-880, 1980.
36. Clauer, C.R., R.L. McPherron, and M.G. Kivelson, Uncertainty in ring current parameters due to the quiet magnetic field variability at midlatitudes, J. Geophys. Res., 85(A2), 633-643, 1980.

37. Rostoker, G., S.-I. Akasofu, J. Foster, R.A. Greenwald, Y. Kamide, K. Kawasaki, A.T.Y. Lui, R.L. McPherron, and C.T. Russell, Magnetospheric substorms--definition and signatures, J. Geophys. Res., 85(A4), 1663-1668, 1980.
38. Clauer, C.T., and R.L. McPherron, The relative importance of the interplanetary electric field and magnetospheric substorms on partial ring current development, J. Geophys. Res., 85(A12), 6747-6759, 1980.
39. Takahashi, K., R.L. McPherron, E.W. Greenstadt, and C.W. Arthur, Factors controlling the occurrence of Pc 3 magnetic pulsations at synchronous orbit, J. Geophys. Res., 86(A7), 5472-5484, 1981.
40. Sakurai, T. and R.L. McPherron, Satellite observations of Pi 2 activity at synchronous orbit, J. Geophys. Res., 88(A9), 7015-7027, 1983.
41. Greenstadt, E.W., R.L. McPherron, and K. Takahashi, Solar wind control of daytime, midperiod geomagnetic pulsations, J. Geomagn. Geoelectr., 32, Suppl. II, SII89-SII-110, 1980.
42. McPherron, R.L., Substorm-associated micropulsations at synchronous orbit, J. Geomagn. Geoelectr., 32, Supp. II, SII57-SII73, 1980.
43. Frank, L.A., R.L. McPherron, R.J. De Coster, B.G. Burek, K.L. Ackerson, and C.T. Russell, Field-aligned currents in the earth's magnetotail, J. Geophys. Res., 86(A21), 687-700, 1981.
44. Clauer, C.R., R.L. McPherron, C.A. Searls, M.G. Kivelson, Solar wind control of auroral zone geomagnetic activity, Geophys. Res. Lett., 8(8), 915-918, 1981.
45. Fraser, B.J., and R.L. McPherron, Pc 1-2 magnetic pulsation spectra and heavy ion effects at synchronous orbit: ATS 6 results, J. Geophys. Res., 87(A6), 4560-4566, 1982.
46. Kokubun, S., and R.L. McPherron, Substorm signatures at synchronous altitudes, J. Geophys. Res., 86(A13), 11265-11277, 1981.
47. Takahashi, K., and R.L. McPherron, Harmonic structure of Pc 3-4 pulsations, J. Geophys. Res., 87(A3), 1504-1516, 1982.
48. Clauer, C.R., R.L. McPherron, C. Searls, Solar wind control of the low-latitude asymmetric magnetic disturbance field, J. Geophys. Res., 88(A4), 2123-2130, 1983.
49. Greenstadt, E.W., R.L. McPherron, M. Hoppe, R.R. Anderson, and F.L. Scarf, A storm-time, Pc 5 event observed in the outer magnetosphere by ISEE 1 and 2: Wave Properties, to be submitted to J. Geophys. Res., 1985.

50. Rostoker, G., S.-I. Akasofu, W. Baumjohann, Y. Kamide, and R.L. McPherron, The roles of direct input of energy from the solar wind and unloading of stored magnetotail energy in driving magnetospheric substorms, revised manuscript to be submitted to J. Geophys. Res., 1985.
51. Sakurai, T., R.L. McPherron, and Y. Tonegawa, Magnetic pulsations associated with SSC observed at synchronous orbit, to be submitted to J. Geophys. Res., 1985.
52. Takahashi, K., and R.L. McPherron, Dynamic spectral analysis of magnetic pulsation, unpublished report, September 1982.
53. Takahashi, K., R.L. McPherron, and W.J. Hughes, Multi-spacecraft observations of the harmonic structure of Pc 3-4 pulsations, J. Geophys. Res., 89(A8), 6758-6774, 1984.
54. Takahashi, K., R.L. McPherron, and T. Terasawa, Dependence of the spectrum of Pc 3-4 pulsations on the interplanetary magnetic field, J. Geophys. Res., 89(A5), 2770-2780, 1984.
55. Takahashi, K., and R.L. McPherron, A reexamination of ATS 6 magnetometer data for radially polarized Pc 3 magnetic pulsations, J. Geophys. Res., 88(A12), 10223-10266, 1983.
56. Greenstadt, E.W., M.M. Mellott, R.L. McPherron, and C.T. Russell, Transfer of pulsation-related wave activity across the magnetopause: Observations of corresponding spectra by ISEE-1 and ISEE-2, Geophys. Res. Lett., 10(8), 659-662, 1983.
57. Tonegawa, Y., H. Fukunishi, T. Hirasawa, R.L. McPherron, T. Sakurai, and Y. Kato, Spectral characteristics of Pc 3 and Pc 4/5 magnetic pulsation bands observed near L=6, J. Geophys. Res., 89(A11), 9720-9730, 1984.
58. Bargatze, L.F., D.N. Baker, R.L. McPherron, and E.W. Hones, Jr., Magnetospheric response for many levels of geomagnetic activity, revised manuscript to be submitted to J. Geophys. Res., 1985.
59. Fraser, B.J., and R.L. McPherron, Heavy ion concentrations at synchronous orbit determined from Pc 1-2 pulsation wave spectra, to be submitted to J. Geophys. Res., 1985.
60. Fraser, B.J., and R.L. McPherron, Observation of  $O^+$  heavy ion effects in Pc 2 pulsation wave spectra, to be submitted to J. Geophys. Res., 1985.
61. Fraser, B.J., and R.L. McPherron, Short time variations in heavy ion ( $He^+$ ,  $O^+$ ) properties observed by Pc 1-2 pulsations at synchronous orbit, to be submitted to J. Geophys. Res., 1985.
62. McPherron, R.L., Final report on ONR Grant N00014-75-C-0396, Submitted to the Office of Naval Research, January 1983.

63. Baker, D.N., S.I. Akasofu, W. Baumjohann, J.W. Bieber, D.H. Fairfield, E.W. Hones, Jr., B. Mauk, R.L. McPherron, T.E. Moore. Substorms in the magnetosphere, Chapter 8 in Solar Terrestrial Physics: Present and Future, edited by D.M. Butler and K. Papadopoulos, NASA Reference Pub. 1120, 1984.
  64. McPherron, R.L., and R.H. Manka, Dynamics of the 1054 UT, March 22, 1979, substorm event: CDAW-6, J. Geophys. Res., in press, February 1985.
  65. McPherron, R.L., Williams Committee Report, An example of a research data base, unpublished report, March 1983.
  66. Takahashi, K. and R.L. McPherron, Standing hydromagnetic oscillations in the magnetosphere, Planet. Space Sci., 32(11), 1343-1359, 1984.
- THE FOLLOWING CITATIONS HAVE BEEN ADDED SINCE LAST YEAR
67. McPherron, R.L., Final report on ONR Grant N00014-84-K-0158, submitted to the Office of Naval Research, December, 1984.
  68. McPherron, R.L., R.A. Fay, C.R. Garrity, L.F. Bargatze, D.N. Baker, C.R. Clauer, and C. Searls, Coupling of the solar wind to measures of magnetic activity, Proc. Conf. Achievements of the IMS, 26-28 June 1984, Graz, Austria, ESA SP-217, September 1984.
  69. Bargatze, L.F., R.L. McPherron, D.N. Baker, and E.W. Hones, Jr., The application of dimensional analysis to the problems of solar wind-magnetosphere energy coupling, Proc. Conf. Achievements of the IMS, 26-28 June 1984, Graz, Austria, ESA SP-217, September 1984.
  70. Barfield, J.N., C.S. Lin, and R.L. McPherron, Observations of magnetic field perturbations at GOES 2 and GOES 3 during the March 22, 1979 substorms: CDAW-6 analysis, J. Geophys. Res., in press, February 1985.
  71. Baker, D.N., T.A. Fritz, R.L. McPherron, D.H. Fairfield, Y. Kamide, and W. Baumjohann, Magnetotail energy storage and release during the CDAW-6 substorm analysis intervals, J. Geophys. Res., in press, February 1985.
  72. Fritz, T.A., D.N. Baker, R.L. McPherron, W. Lennartsson, Implications of the 1100 UT, March 22, 1979, CDAW-6 substorm event for the role of magnetic reconnection in the geomagnetic tail, p. 203-207 in Magnetic Reconnection in Space and Laboratory Plasmas, Geophys. Monograph No. 30, edited by E.W. Hones, Jr., American Geophysical Union, Washington, D.C., 1984.
  73. Kamide, Y. H.W. Kroel, B.A. Hausman, R.L. McPherron, S.-I. Akasofu, A.D. Richmond, P.H. Reiff, and S. Matsushita, Numerical modeling of ionospheric parameters from global IMS magnetometer data for the CDAW-6 intervals, Report UAG-88, WDC-A for Solar Terrestrial Physics, Boulder, Colorado, November 1983.

74. McPherron, R.L. and C.T. Russell, CDAW-6: Changes in the tail magnetic field during the 1054 UT, March 22, 1979, substorm, to be submitted to J. Geophys. Res., 1985.

END

FILMED

3 - 86

DTIC